




Extracellular Zn²⁺ Influx into Nigral Dopaminergic Neurons Plays a Key Role for Pathogenesis of 6-Hydroxydopamine-Induced Parkinson's Disease in Rats

Haruna Tamano¹ · Ryusuke Nishio¹ · Hiroki Morioka¹ · Atsushi Takeda¹ 

Received: 20 December 2017 / Accepted: 10 April 2018 / Published online: 29 April 2018
© Springer Science+Business Media, LLC, part of Springer Nature 2018

Abstract

Parkinson's disease (PD) is a progressive neurological disease characterized by a selective loss of nigrostriatal dopaminergic neurons. The exact cause of the neuronal loss remains unclear. Here, we report a unique mechanism of nigrostriatal dopaminergic neurodegeneration, in which extracellular Zn²⁺ influx plays a key role for PD pathogenesis induced with 6-hydroxydopamine (6-OHDA) in rats. 6-OHDA rapidly increased intracellular Zn²⁺ only in the substantia nigra pars compacta (SNpc) of brain slices and this increase was blocked in the presence of CaEDTA, an extracellular Zn²⁺ chelator, and 6-cyano-7-nitroquinoxaline-2,3-dione (CNQX), an α -amino-3-hydroxy-5-methyl-4-isoxazolepropionate (AMPA) receptor antagonist, indicating that 6-OHDA rapidly increases extracellular Zn²⁺ influx via AMPA receptor activation in the SNpc. Extracellular Zn²⁺ concentration was decreased under in vivo SNpc perfusion with 6-OHDA and this decrease was blocked by co-perfusion with CNQX, supporting 6-OHDA-induced Zn²⁺ influx via AMPA receptor activation in the SNpc. Interestingly, both 6-OHDA-induced loss of nigrostriatal dopaminergic neurons and turning behavior to apomorphine were ameliorated by co-injection of intracellular Zn²⁺ chelators, i.e., ZnAF-2DA and *N,N,N',N'*-Tetrakis(2-pyridylmethyl)ethylenediamine (TPEN). Co-injection of TPEN into the SNpc blocked 6-OHDA-induced increase in intracellular Zn²⁺ but not in intracellular Ca²⁺. These results suggest that the rapid influx of extracellular Zn²⁺ into dopaminergic neurons via AMPA receptor activation in the SNpc induces nigrostriatal dopaminergic neurodegeneration, resulting in 6-OHDA-induced PD in rats.

Keywords Zinc · Dopaminergic neuron · Substantia nigra · 6-hydroxydopamine · Parkinson's disease

Introduction

Parkinson's disease (PD) is a very common age-related disease affecting more than 1% of the population over 60 years of age. The majority (~90%) of PD is sporadic and aging is the major risk factor [1]. PD is one of the most common neurodegenerative diseases and characterized by a selective loss of dopaminergic neurons in the substantia nigra pars compacta (SNpc), a mesencephalic nucleus included in the basal ganglia circuitry, which is responsive for the regulation of voluntary movement. However, the exact cause of the neuronal loss remains unclear [2].

Glutamate excitotoxicity is the pathological process through which neurons are damaged and killed after excess activation of glutamate receptors. Glutamate excitotoxicity is due to intracellular processes such as Ca²⁺ overload and bioenergetic changes, which induce oxidative stress and apoptosis. This excitotoxicity is known as a final common pathway for neuronal death and is observed in many neurological diseases including PD [3–6].

In the basal ganglia, the projection from the subthalamic nucleus (STN) to the SNpc is glutamatergic and the SNpc is also innervated from the amygdala via glutamatergic neurotransmitter system [7, 8]. Dopaminergic neurons express glutamate receptors in the SNpc [9]. It has been postulated that excess activation of glutamate receptors on dopaminergic neurons in the SNpc may be involved in pathophysiology of PD [10–14].

The influx of extracellular Ca²⁺ through *N*-methyl-D-aspartate (NMDA) receptors plays a crucial role in glutamate excitotoxicity in cortical and hippocampal neurons [15, 16]. Even in dopaminergic neurons where the mechanism of

✉ Atsushi Takeda
takedaa@u-shizuoka-ken.ac.jp

¹ Department of Neurophysiology, School of Pharmaceutical Sciences, University of Shizuoka, 52-1 Yada, Suruga-ku, Shizuoka 422-8526, Japan

glutamate excitotoxicity is poorly understood, Ca^{2+} influx through NMDA receptors has been believed to be a trigger for neuronal death [8, 17]. In contrast, it is recognizing that most of the death signaling associated with neurological conditions is mediated by not only Ca^{2+} but also Zn^{2+} [18–20]. Extracellular Zn^{2+} influx, which is dynamically linked with Zn^{2+} release from zincergic neuron, a subclass of glutamatergic neurons, is particularly important in causing the selective and delayed degeneration of hippocampal CA1 pyramidal neurons in transient global ischemia [21]. However, glutamatergic neurons are non-zincergic in the SNpc and do not contain zinc in the presynaptic vesicles [22]. Thus, it is estimated that extracellular Zn^{2+} concentration is not dynamically increased by glutamatergic synapse excitation in the SNpc unlike the hippocampus.

In human neuroblastoma SH-SY5Y cells, a dopaminergic neuronal cell line, Zn^{2+} -induced neurotoxicity occurs via Zn^{2+} -permeable transient receptor potential melastatin 7 (TRPM7) channel at the micromolar range of extracellular Zn^{2+} concentration [23]. Yang et al. report that cell death caused by the synergistic effects of micromolar Zn^{2+} and dopamine is observed in PC12 via a stress sensor gene Gadd45b. They suggest that Zn^{2+} and dopamine are implicated in the degeneration of dopaminergic neurons [24]. However, the micromolar range of extracellular Zn^{2+} is improbable in the SNpc in vivo, judging from the estimated basal concentration (~ 10 nM) of extracellular Zn^{2+} in the hippocampus [25]. On the other hand, Lee et al. report that cytosolic Zn^{2+} accumulation is observed in degenerating dopaminergic neurons after treatment with 1-methyl-4-phenyl-1,2,3,6-tetrahydropyridine (MPTP). They suppose that cytosolic Zn^{2+} accumulation is an indicator of degenerating dopaminergic neurons in animal models of PD [26]. Therefore, it is important to clarify the significance of cytosolic Zn^{2+} toxicity and its origin in nigrostriatal dopaminergic neurodegeneration.

Here, we report a unique mechanism of nigrostriatal dopaminergic neurodegeneration, in which extracellular Zn^{2+} influx plays a key role for PD pathogenesis induced with 6-hydroxydopamine (6-OHDA) in rats.

Materials and Methods

Animals and Chemicals

Male Wistar rats (6–12 weeks of age) were purchased from Japan SLC (Hamamatsu, Japan). Rats were housed under the standard laboratory conditions (23 ± 1 °C, $55 \pm 5\%$ humidity) and had access to tap water and food ad libitum. All the experiments were performed in accordance with the Guidelines for the Care and Use of Laboratory Animals of the University of Shizuoka that refers to the American Association for Laboratory Animals Science and the guidelines laid down by

the NIH (NIH Guide for the Care and Use of Laboratory Animals) in the USA. The Ethics Committee for Experimental Animals in the University of Shizuoka has approved this work.

ZnAF-2 and ZnAF-2DA, membrane-impermeable and membrane-permeable Zn^{2+} fluorescence probes, were kindly supplied from Sekisui Medical Co., LTD (Hachimantai, Japan). ZnAF-2DA is taken up into the cells through the cell membrane and is hydrolyzed by esterase in the cytosol to yield ZnAF-2, which cannot permeate the cell membrane [27, 28]. ZnAF-2 is selectively bound to Zn^{2+} , but not bound to other divalent cations such as Ca^{2+} , Mg^{2+} , and Cu^{2+} [24]. Calcium orange acetoxymethyl ester (AM), a membrane-permeable Ca^{2+} indicator, was purchased from Molecular Probes, Inc. (Eugene, OR). These fluorescence indicators were dissolved in dimethyl sulfoxide (DMSO) and then diluted to artificial cerebrospinal fluid (ACSF) containing 119 mM NaCl, 2.5 mM KCl, 1.3 mM MgSO_4 , 1.0 mM NaH_2PO_4 , 2.5 mM CaCl_2 , 26.2 mM NaHCO_3 , and 11 mM D-glucose (pH 7.3).

In Vivo Microdialysis

The rats were anesthetized with chloral hydrate (400 mg/kg) and individually placed in a stereotaxic apparatus. The skull was exposed, a burr hole was drilled, and a microdialysis probe (1-mm membrane, Eicom, Kyoto) was inserted into the right SNpc (5.3 mm posterior to the bregma, 2.0 mm lateral, 7.8 mm inferior to the dura). The SNpc was preperfused with artificial cerebrospinal fluid (ACSF) (127 mM NaCl, 2.5 mM KCl, 1.3 mM CaCl_2 , 0.9 mM MgCl_2 , 1.2 mM Na_2HPO_4 , 21 mM NaHCO_3 , and 3.4 mM D-glucose, pH 7.3) containing 0.1% ascorbic acid at 2.0 $\mu\text{l}/\text{min}$ for 120 min to stabilize the region, perfused with ACSF containing 0.1% ascorbic acid or ACSF containing 0.1% ascorbic acid + 50 μM 6-cyano-7-nitroquinoxaline-2,3-dione (CNQX), an α -amino-3-hydroxy-5-methyl-4-isoxazolepropionate (AMPA) receptor antagonist, for 60 min in the same manner to determine the basal concentration of extracellular Zn^{2+} , and then perfused with 0.8 mM 6-OHDA in ACSF containing 0.1% ascorbic acid or 0.8 mM 6-OHDA + 50 μM CNQX in ACSF containing 0.1% ascorbic acid, respectively, for 60 min. The perfusate was collected for 60 min and 1 μM ZnAF-2 (50 μl) was added to aliquot of the perfusate (10 μl). The fluorescence of ZnAF-2 (excitation/emission, 485/535 nm) was measured using a plate reader ARVO sx (Perkin Elmer, USA).

In Vivo Dynamics of Intracellular Zn^{2+} and Ca^{2+}

The rats were anesthetized with chloral hydrate (400 mg/kg) and individually placed in a stereotaxic apparatus. The skull was exposed, a burr hole was drilled, and injection cannulae (internal diameter, 0.15 mm; outer diameter, 0.35 mm) were carefully and slowly inserted into the right and left SNpc

(5.3 mm posterior to the bregma, 2.0 mm lateral, 7.0 mm inferior to the dura) to avoid cellular damages. Thirty minutes after the surgical operation, 6-OHDA (8 mM) or 6-OHDA (8 mM) + *N,N,N',N'*-Tetrakis(2-pyridylmethyl)ethylenediamine (TPEN) (100 μ M), a membrane-permeable Zn^{2+} chelator, in saline containing 0.1% ascorbic acid + ZnAF-2DA (100 μ M) or in saline containing 0.1% ascorbic acid + calcium orange AM (50 μ M) were bilaterally injected into the SNpc via cannulae at the rate of 0.5 μ l/min for 8 min. Ten minutes after injection, the injection cannulas were slowly pulled out the brain in about 10 min and the rats were decapitated. The brain was quickly removed and immersed in ice-cold choline-ACSF containing 124 mM choline chloride, 2.5 mM KCl, 2.5 mM $MgCl_2$, 1.25 mM NaH_2PO_4 , 0.5 mM $CaCl_2$, 26 mM $NaHCO_3$, and 10 mM glucose (pH 7.3) to avoid neuronal excitation. Coronal brain slices (400 μ m) were prepared using a vibratome ZERO-1 (Dosaka, Kyoto, Japan) in an ice-cold choline-ACSF and maintained in an ice-cold choline-ACSF for 30 min. The brain slices were immersed in ACSF for 15 min and transferred to a recording chamber filled with ACSF. The fluorescence of ZnAF-2 (laser, 488.4 nm; emission, 500–550 nm) and calcium orange (laser, 561.4 nm; emission, 570–620 nm) was measured with a confocal laser scanning microscopic system (Nikon A1 confocal microscopes, Nikon Corp.). Region of interest was set in the SNpc.

In Vitro Dynamics of Extracellular Zn^{2+}

The brain was quickly removed from rats under anesthesia with chloral hydrate and immersed in ice-cold choline-ACSF. Coronal brain slices (400 μ m) were prepared and maintained in ice-cold choline-ACSF for 15 min. To assess intracellular levels of Zn^{2+} , brain slices were placed for 30 min in 10 μ M ZnAF-2DA in ACSF, rinsed in choline-ACSF for 20 min, placed in a chamber filled with 8 mM 6-OHDA, 8 mM 6-OHDA + 10 mM CaEDTA, a membrane-impermeable Zn^{2+} chelator, or 8 mM 6-OHDA + 10 μ M CNQX in ACSF containing 10 nM $ZnCl_2$ for 10 min, rinsed in choline-ACSF for 15 min, and transferred to a recording chamber filled with ACSF. The fluorescence of ZnAF-2 was measured in the same manner.

Behavioral Studies

As described in the section of “[In vivo dynamics of intracellular \$Zn^{2+}\$ and \$Ca^{2+}\$ ”](#), an injection cannula was inserted into the right SNpc and 6-OHDA (8 mM), 6-OHDA (8 mM) + ZnAF-2DA (200 μ M), or 6-OHDA (8 mM) + TREN (100 μ M) in saline containing 0.1% ascorbic acid was unilaterally injected into the SNpc via the cannula at the rate of 0.5 μ l/min for 8 min. Ten minutes after injection, the injection cannula was slowly pulled out the brain in about 10 min. One and 2 weeks later, the rats were subcutaneously injected with

apomorphine (0.5 mg/kg) and turning behavior in response to apomorphine was measured for 30 min after the start of the turning behavior.

Tyrosine Hydroxylase Immunostaining

The rats were anesthetized and perfused with ice-cold 4% paraformaldehyde in PBS after the behavioral studies were finished, followed by removal of the brain and overnight fixation in 4% paraformaldehyde in PBS at 4 °C. Fixed brains were cryopreserved in 30% sucrose in PBS for 2 days and frozen in Tissue-Tek optimal cutting temperature embedding medium. Coronal brain slices (30 μ m) were prepared at –20 °C in a cryostat, picked up on slides, and adhered at room temperature for 30 min. For immunostaining, slides were incubated in blocking solution (3% BSA, 0.1% Triton X-100 in PBS) for 1 h and rinsed with PBS for 5 min followed by overnight incubation with anti-tyrosine hydroxylase antibody (Abcam) at 4 °C. Slides were rinsed with PBS for 5 min and incubated in blocking buffer containing Alexa Fluor 633 goat anti-rabbit secondary antibody (ThermoFisher) for 3 h at room temperature. Following six rinses in PBS for 5 min, slides were mounted with Prolong Gold antifade reagent and placed for 24 h at 4 °C. Alexa Fluor 633 fluorescence was measured in the SNpc and the striatum using a confocal laser scanning microscopic system.

Data Analysis

For statistical analysis, Student's *t* test was used for comparison of the means of paired or unpaired data. For multiple comparisons, differences between treatments were assessed by one-way ANOVA followed by post hoc testing using the Tukey test (the statistical software, GraphPad Prism 5). A value of $p < 0.05$ was considered significant. Data were expressed as means \pm standard error. The results of statistical analysis are described in each figure legend.

Results

6-OHDA Increases Extracellular Zn^{2+} Influx in the SNpc

6-OHDA is a classic animal model of PD [29]. Reactive oxygen species (ROS) derived from 6-OHDA uptake and intraneuronal autooxidation, extracellular 6-OHDA autooxidation, and microglial activation may be involved in the mechanisms responsible for 6-OHDA-induced dopaminergic degeneration [30]. We examined the idea that 6-OHDA-mediated ROS production modifies intracellular Zn^{2+} dynamics in nigral dopaminergic neurons. 6-OHDA rapidly increased intracellular Zn^{2+} in the SNpc of brain slices after 10-min incubation with 6-OHDA in ACSF containing 10 nM

Zn^{2+} , an estimated basal concentration of extracellular Zn^{2+} [25], but not in the substantia nigra pars reticulata (SNpr) and other midbrain area (deep mesencephalic nuclei and/or parabrachial pigmented nuclei) (Fig. 1a, b) and this increase was blocked in the presence of CaEDTA, an extracellular Zn^{2+} chelator and CNQX, an AMPA receptor antagonist (Fig. 1a, c).

An *in vivo* microdialysis experiment indicated extracellular Zn^{2+} concentration in the perfusate, which was determined with ZnAF-2, was decreased under SNpc perfusion with 6-OHDA, while this decrease was blocked by co-perfusion with CNQX (Fig. 2). Unfortunately, extracellular glutamate concentration was disturbed by the presence of 6-OHDA in the perfusate (data not shown).

Intracellular Zn^{2+} Chelators Ameliorate 6-OHDA-Induced Neurodegeneration

Turning behavior in response to apomorphine, an index of behavioral abnormality of 6-OHDA-induced PD in rats was ameliorated by co-injection of membrane-permeable Zn^{2+} chelators, i.e., ZnAF-2DA and TPEN 1 and 2 weeks after 6-OHDA injection (Fig. 3).

6-OHDA-induced loss of nigrostriatal dopaminergic neurons was determined by tyrosine hydroxylase immunostaining after the behavioral test was finished. Staining intensity was drastically reduced in the ipsilateral SNpc (Fig. 4a, c) and the striatum (Fig. 4b, d). However, the reductions were also ameliorated by co-injection of ZnAF-2DA and TPEN.

TPEN Blocks 6-OHDA-Induced Increase in Intracellular Zn^{2+} , but not in Intracellular Ca^{2+}

To assess the involvement of the influx of Zn^{2+} and Ca^{2+} in behavioral abnormality via 6-OHDA-induced nigrostriatal dopaminergic neurodegeneration, *in vivo* dynamics of intracellular Zn^{2+} and Ca^{2+} was captured 30 min after the start of 6-OHDA injection into the SNpc (Fig. 5a). Both intracellular Zn^{2+} and Ca^{2+} were increased in the SNpc, while TPEN blocked the increase in intracellular Zn^{2+} (Fig. 5b), but not in intracellular Ca^{2+} (Fig. 5c).

Discussion

Evidence has pinpointed Ca^{2+} as the major determinant of ischemic neuronal death, based on Ca^{2+} imaging experiments

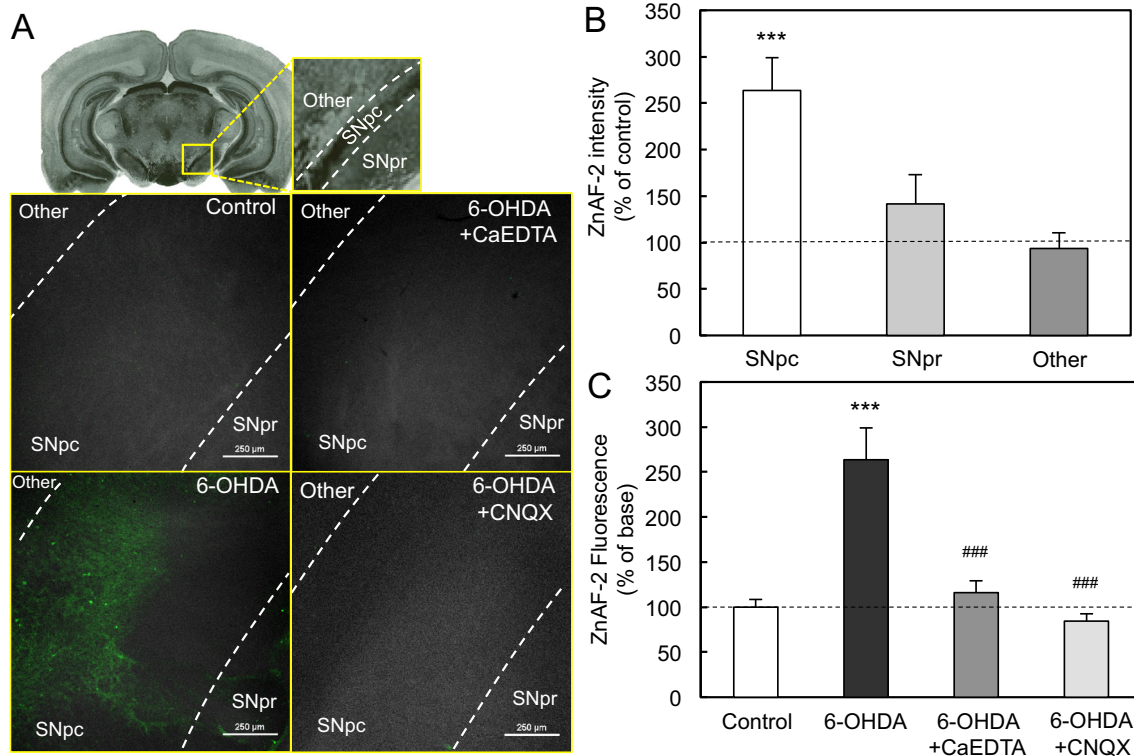


Fig. 1 6-OHDA increases intracellular Zn^{2+} concentration in the SNpc *in vitro*. Brain slices loaded with ZnAF-2DA were immersed in vehicle (control), 8 mM 6-OHDA in ACSF, 8 mM 6-OHDA + 10 mM CaEDTA in ACSF, or 8 mM 6-OHDA + 10 μ M CNQX in ACSF for 10 min. **a** Intracellular ZnAF-2 fluorescence was imaged in the SNpc, SNpr, and other midbrain area. The SN and magnified SN are shown in the coronal

brain image (upper side) for better understanding the area of the SNpc where it is surrounded by the white dotted line. **b, c** Each bar and line represents the ratio of ZnAF-2 fluorescence intensity to the control ZnAF-2 fluorescence intensity, which was expressed as 100%. *** $p < 0.001$ vs. control, ### $p < 0.001$ vs. 6-OHDA group (Tukey's test)

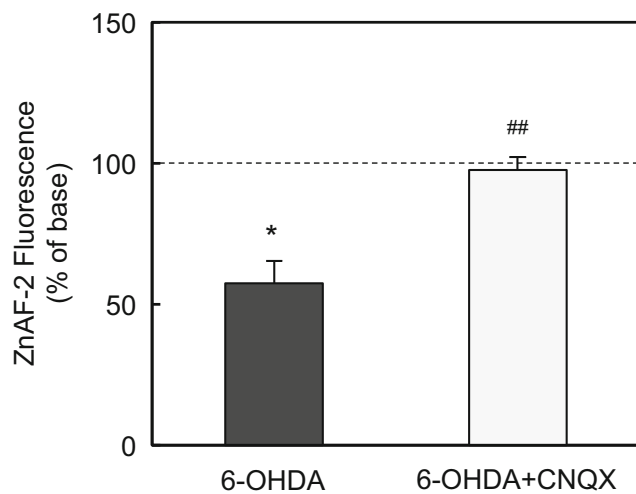


Fig. 2 6-OHDA decreases extracellular Zn^{2+} concentration in the SNpc in vivo. The SNpc was perfused with ACSF containing 0.1% ascorbic acid or ACSF containing 0.1% ascorbic acid + 50 μ M CNQX for 60 min at 2.0 μ l/min to determine the basal concentration of extracellular Zn^{2+} and then perfused with 0.8 mM 6-OHDA in ACSF containing 0.1% ascorbic acid or 0.8 mM 6-OHDA + 50 μ M CNQX in ACSF containing 0.1% ascorbic acid, respectively, for 60 min. Zn^{2+} concentration in the perfusate was determined with ZnAF-2. Each bar and line represents the ratio of ZnAF-2 fluorescence intensity to the basal ZnAF-2 fluorescence intensity, which was expressed as 100%. * p < 0.001 vs. the basal level, ## p < 0.01 vs. 6-OHDA group (t test)

that use Ca^{2+} fluorescence probes or the neuroprotection offered by Ca^{2+} chelators. However, all of Ca^{2+} fluorescence probes and Ca^{2+} chelators are not Ca^{2+} selective, and they indeed show a higher affinity for Zn^{2+} [19, 31]. On the other hand, extracellular Zn^{2+} permeates NMDA receptors and voltage-dependent Ca^{2+} Channels, while it preferentially passes through Ca^{2+} - and Zn^{2+} -permeable GluR2-lacking AMPA receptors [18, 32]. Ca^{2+} - and Zn^{2+} -permeable GluR2-lacking AMPA receptors are involved in synaptically released Zn^{2+} -mediated neurodegeneration in the hippocampal CA1 and CA3 [33–35]. Nigral dopaminergic neurons are not innervated by zincergic neurons unlike hippocampal pyramidal neurons [22]. Thus, extracellular Zn^{2+} concentration is not significantly increased by glutamatergic neuron excitation in the SNpc. On the other hand, 6-OHDA has been shown to produce endogenously in patients suffering from PD [36, 37] and to increase intracellular Zn^{2+} release and accumulation via ROS production [38, 39]. Intracellular (cytosolic) Zn^{2+} concentration is estimated to be considerably less than 1 nM in nigral dopaminergic neurons [40, 41]. We postulated that nigral dopaminergic neurons are sensitive to intracellular Zn^{2+} dysregulation and tested a unique mechanism of nigrostriatal dopaminergic neurodegeneration, in which extracellular Zn^{2+} dynamics plays a key role for PD pathogenesis induced with 6-OHDA in rats.

6-OHDA rapidly increased intracellular Zn^{2+} only in the SNpc of brain slices after 10-min incubation with 6-OHDA in

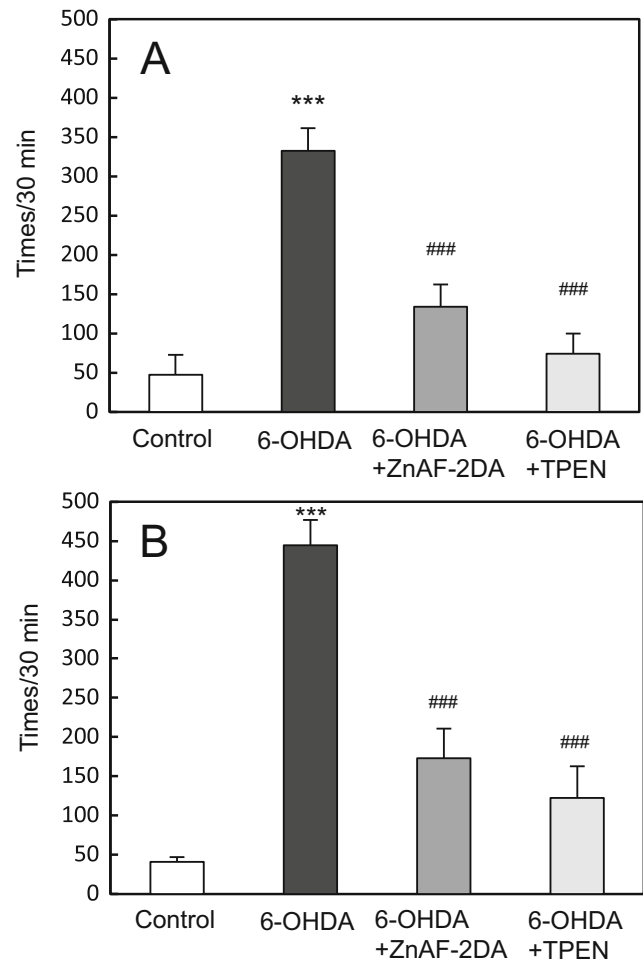


Fig. 3 Turning behavior to apomorphine after injection of 6-OHDA into the SNpc. Vehicle (control), 6-OHDA (8 mM), 6-OHDA (8 mM) + ZnAF-2DA (200 μ M), or 6-OHDA (8 mM) + TPEN (100 μ M) in saline containing 0.1% ascorbic acid was unilaterally injected into the SNpc. One (a) and 2 (b) weeks later, the rats were subcutaneously injected with apomorphine (0.5 mg/kg) and turning behavior (the number of times) in response to apomorphine was measured for 30 min after the start of the turning behavior. *** p < 0.001 vs. control, ### p < 0.001 vs. 6-OHDA group (Tukey's test). *** p < 0.001 vs. control, ### p < 0.001 vs. 6-OHDA group (Tukey's test)

ACSF containing 10 nM Zn^{2+} while this increase was blocked in the presence of CaEDTA and CNQX, indicating that 6-OHDA rapidly increases extracellular Zn^{2+} influx via AMPA receptor activation in the SNpc. Extracellular Zn^{2+} concentration was decreased under in vivo SNpc perfusion with 6-OHDA and this decrease was blocked by co-perfusion with CNQX, supporting 6-OHDA-induced Zn^{2+} influx via AMPA receptor activation in the SNpc. These results suggest that 6-OHDA-mediated ROS production increases extracellular Zn^{2+} influx into dopaminergic neurons via AMPA receptor activation in the SNpc. It is likely that 6-OHDA-mediated ROS production increases glutamate release from neuron terminals in the SNpc. 6-OHDA is taken up into dopaminergic neurons through dopamine transporters and

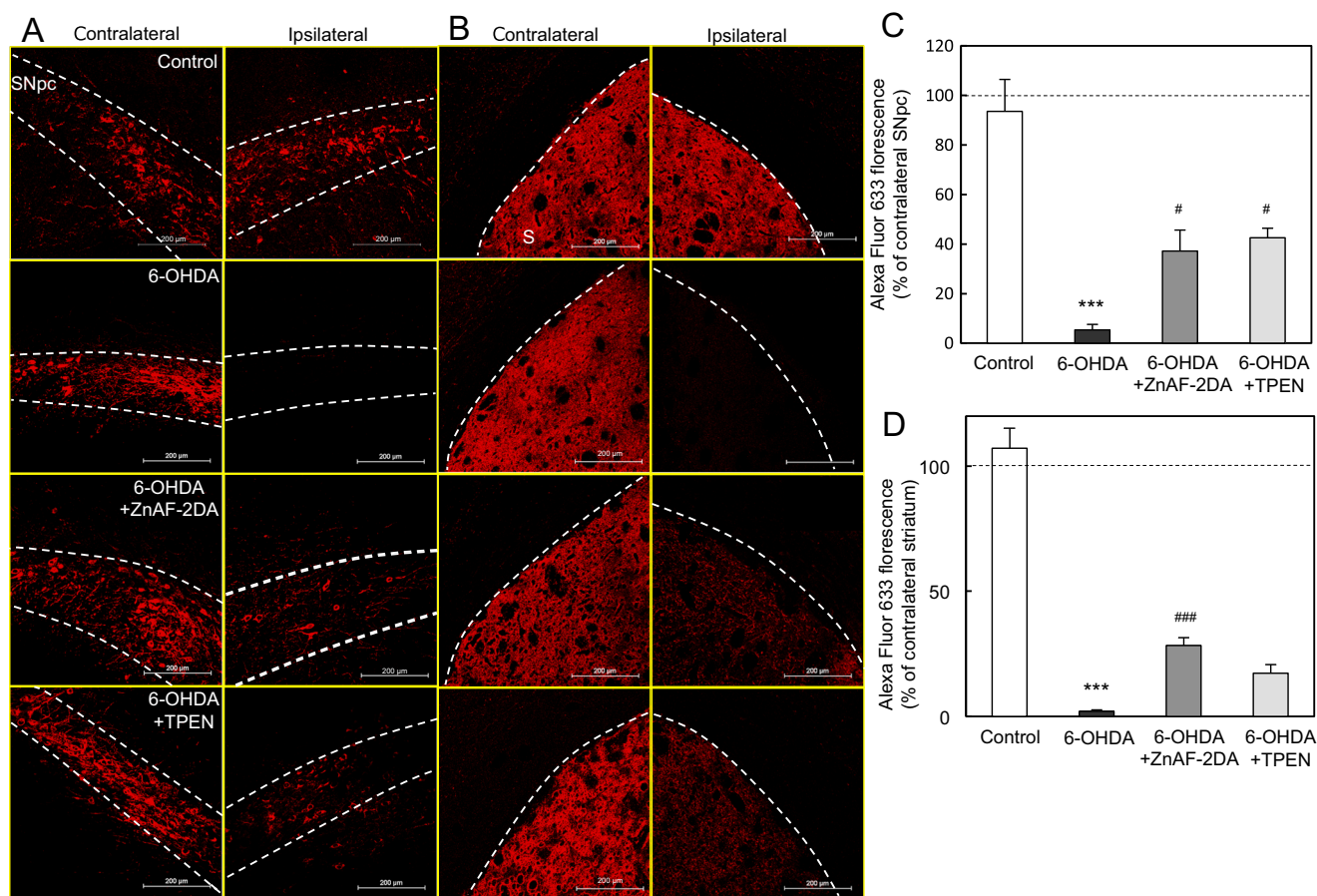


Fig. 4 Neuronal loss in the SNpc and striatum after injection of 6-OHDA into the SNpc. Brain slices were prepared from the rats after the behavioral test was finished and tyrosine hydroxylase immunostaining with Alexa Fluor 633 fluorescence was performed in the SNpc (a) and the striatum (S) where it was surrounded by the white dotted line. Each bar

and line represents the ratio of Alexa Fluor 633 fluorescence intensity to Alexa Fluor 633 fluorescence intensity in the control contralateral SNpc (c) and striatum (d), which was expressed as 100%. *** $p < 0.001$ vs. control, # $p < 0.05$, ### $p < 0.001$, vs. 6-OHDA group (Tukey's test)

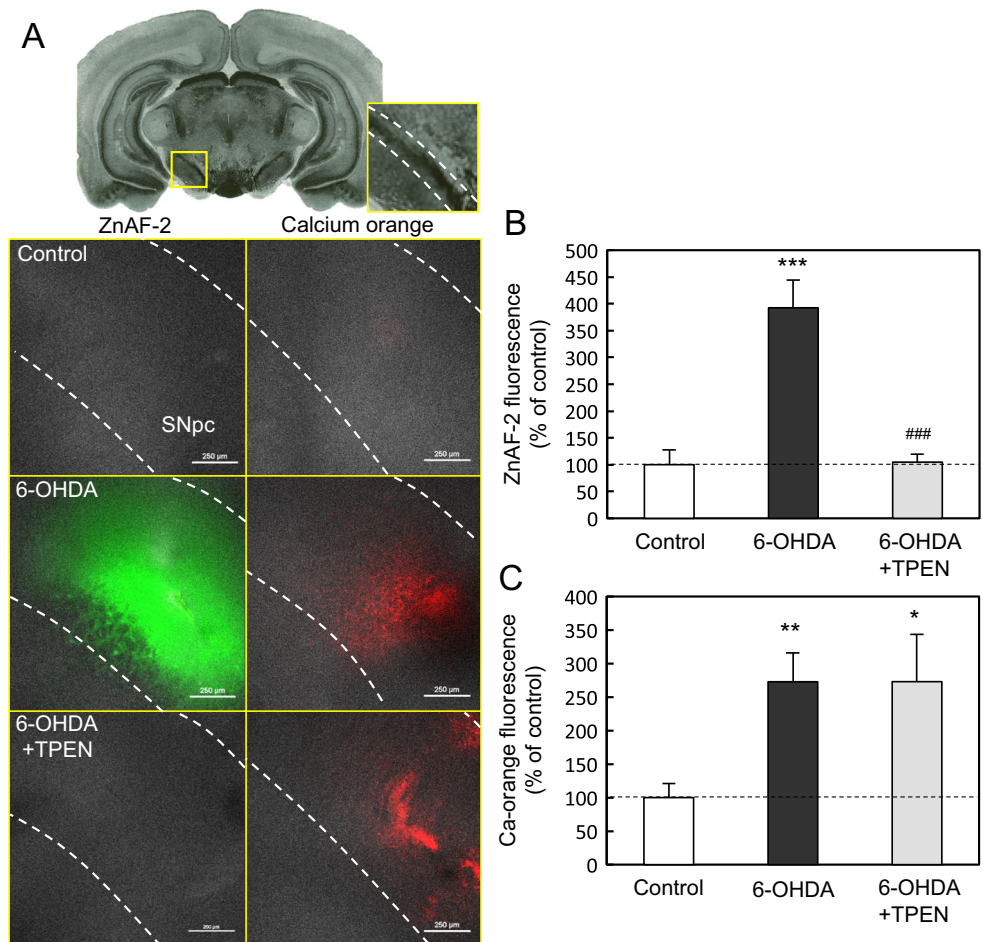
rapidly produces ROS in the intracellular compartment, in addition to ROS production by autoxidation in the extracellular compartment [42]. It is possible that both extracellular ROS and ROS in dopaminergic neurons, which is retrogradely transported, are taken up into glutamatergic neuron terminals and induce glutamate release. The data that 6-OHDA-induced increase in Zn^{2+} influx was selectively observed in the SNpc of brain slices suggest that the rapid Zn^{2+} influx into dopaminergic neurons is due to ROS produced in dopaminergic neurons rather than extracellular ROS.

Next, we examined whether nigrostriatal dopaminergic neurodegeneration induced with 6-OHDA could be due to the rapid increase in intracellular Zn^{2+} . Interestingly, both 6-OHDA-induced loss of nigrostriatal dopaminergic neurons and turning behavior to apomorphine were ameliorated by co-injection of intracellular Zn^{2+} chelators, i.e., ZnAF-2DA and TPEN. Extracellular Zn^{2+} concentration, which is estimated to be approximately 10 nM in the hippocampus [25], was decreased in the SNpc by the rapid Zn^{2+} influx via 6-OHDA-mediated AMPA receptor activation. The finding suggests that

intracellular Zn^{2+} concentration rapidly reaches ~ 10 nM, resulting in neuronal death. The lethal concentration of intracellular Ca^{2+} is micromolar (10–20 μ M) [43], while the present data indicate that the lethal concentration of intracellular Zn^{2+} is much low in the SNpc and that nigral dopaminergic neurons are much vulnerable to intracellular Zn^{2+} dysregulation.

In ischemic neuronal death, acidosis reduces Zn^{2+} binding to metallothioneins, followed by the increase in intracellular Zn^{2+} [44]. Furthermore, mitochondrial dysfunction including ROS generation promotes intracellular Zn^{2+} mobilization, which originates in the mitochondria and metallothioneins [38, 45]. Among metallothionein isoforms, metallothionein III preferentially releases Zn^{2+} under oxidative condition [46]. ROS-mediated TRPM7 (transient receptor potential cation channel subfamily M member 7) activation releases Zn^{2+} from intracellular vesicles after Zn^{2+} overload [47]. In the present study, rapid increase in intracellular Zn^{2+} induced with 6-OHDA was almost completely blocked in the presence of CaEDTA and

Fig. 5 6-OHDA increases intracellular Zn^{2+} in the SNpc but not intracellular Ca^{2+} in vivo. Vehicle (control), 6-OHDA (8 mM), or 6-OHDA (8 mM) + TPEN (100 μ M) in saline containing 0.1% ascorbic acid was bilaterally injected into the SNpc. (a) Intracellular fluorescence of ZnAF-2 and calcium orange was measured in the SNpc where it is surrounded by the white dotted line. Each bar and line represents the ratio of ZnAF-2 (b) and Ca-orange (c) fluorescence intensity to the control fluorescence intensity, which was expressed as 100%. * $p < 0.05$, ** $p < 0.01$, *** $p < 0.001$ vs. control; ### $p < 0.001$ vs. 6-OHDA group (Tukey's test)



CNQX, suggesting that the rapid increase is due to extracellular Zn^{2+} influx but not Zn^{2+} release from metallothioneins and/or internal stores. Although it is possible that Zn^{2+} release from metallothioneins and/or internal stores occurs in the late stage of neurodegeneration, the block of the rapid Zn^{2+} influx via 6-OHDA-mediated ROS production may be an effective strategy for reducing nigrostriatal dopaminergic neurodegeneration in the SNpc.

Co-injection of TPEN into the SNpc blocked 6-OHDA-induced increase in intracellular Zn^{2+} but not in intracellular Ca^{2+} . The present study indicates that 6-OHDA-induced rapid increase in extracellular Zn^{2+} influx into dopaminergic neurons via AMPA receptor activation in the SNpc induces PD via nigrostriatal dopaminergic neurodegeneration. Dopamine is rapidly taken up into dopaminergic neurons via dopamine transporters in the SNpc [48], produces intracellular ROS, and might be metabolized to 6-OHDA [42]. Therefore, 6-OHDA- and dopamine-induced Zn^{2+} influx may be a trigger for dopaminergic neurodegeneration in the SNpc. Characteristics (easiness) of extracellular Zn^{2+} influx may be linked with weakened intracellular Zn^{2+} -buffering in the aged dentate gyrus [49, 50], indicating that vulnerability to intracellular Zn^{2+}

dysregulation is promoted in the brain along with aging. Metabolic disorder of synaptic dopamine might induce intracellular Zn^{2+} dysregulation via ROS production, perhaps followed by pathogenesis of dopaminergic neurodegeneration in the SNpc.

Compliance with Ethical Standards

Conflict of Interest The authors declare that they have no conflict of interest.

References

- de Lau LM, Breteler MM (2006) Epidemiology of Parkinson's disease. *Lancet Neurol* 5:525–535
- Zhai S, Tanimura A, Graves SM, Shen W, Surmeier DJ (2017) Striatal synapses, circuits, and Parkinson's disease. *Curr Opin Neurobiol* 48:9–16
- Danbolt NC (2001) Glutamate uptake. *Prog Neurobiol* 65:1–105
- Dong XX, Wang Y, Qin ZH (2009) Molecular mechanisms of excitotoxicity and their relevance to pathogenesis of neurodegenerative diseases. *Acta Pharmacol Sin* 30:379–387

5. Lai TW, Zhang S, Wang YT (2014) Excitotoxicity and stroke: identifying novel targets for neuroprotection. *Prog Neurobiol* 115:157–188
6. Lewerenz J, Maher P (2015) Chronic glutamate toxicity in neurodegenerative diseases—what is the evidence? *Front Neurosci* 9:469
7. Kita H, Kitai ST (1987) Efferent projections of the subthalamic nucleus in the rat: light and electron microscopic analysis with the PHA-L method. *J Comp Neurol* 260:435–452
8. Ambrosi G, Cerri S, Blandini F (2014) A further update on the role of excitotoxicity in the pathogenesis of Parkinson's disease. *J Neural Transm (Vienna)* 121:849–859
9. Chatha BT, Bernard V, Streit P, Bolam JP (2000) Synaptic localization of ionotropic glutamate receptors in the rat substantia nigra. *Neuroscience* 101:1037–1051
10. Schmidt WJ, Bubser M, Hauber W (1990) Excitatory amino acids and Parkinson's disease. *Trends Neurosci* 13:46–47
11. Difazio MC, Hollingsworth Z, Young AB, Penney JB Jr (1992) Glutamate receptors in the substantia nigra of Parkinson's disease brains. *Neurology* 42:402–406
12. Blandini F, Porter RH, Greenamyre JT (1996) Glutamate and Parkinson's disease. *Mol Neurobiol* 12:73–94
13. Rodriguez MC, Obeso JA, Olanow CW (1998) Subthalamic nucleus-mediated excitotoxicity in Parkinson's disease: a target for neuroprotection. *Ann Neurol* 44:S175–S188
14. Izumi Y, Yamamoto N, Matsuo T, Wakita S, Takeuchi H, Kume T, Katsuki H, Sawada H et al (2009) Vulnerability to glutamate toxicity of dopaminergic neurons is dependent on endogenous dopamine and MAPK activation. *J Neurochem* 110:745–755
15. Choi DW (1988) Glutamate neurotoxicity and diseases of the nervous system. *Neuron* 1:623–634
16. Swann JW, Al-Noori S, Jiang M, Lee CL (2000) Spine loss and other dendritic abnormalities in epilepsy. *Hippocampus* 10:617–625
17. Oster S, Radad K, Scheller D, Hesse M, Balanzew W, Reichmann H, Gille G (2014) Rotigotine protects against glutamate toxicity in primary dopaminergic cell culture. *Eur J Pharmacol* 724:31–42
18. Frederickson CJ, Koh JY, Bush AI (2005) The neurobiology of zinc in health and disease. *Nat Rev Neurosci* 6:449–462
19. Sensi SL, Paoletti P, Bush AI, Sekler I (2009) Zinc in the physiology and pathology of the CNS. *Nat Rev Neurosci* 10:780–791
20. Takeda A, Tamano H (2016) Insight into cognitive decline from $^{2+}Zn^{2+}$ dynamics through extracellular signaling of glutamate and glucocorticoids. *Arch Biochem Biophys* 611:93–99
21. Koh JY, Suh SW, Gwag BJ, He YY, Hsu CY, Choi DW (1996) The role of zinc in selective neuronal death after transient global cerebral ischemia. *Science* 272:1013–1016
22. Frederickson CJ (1989) Neurobiology of zinc and zinc-containing neurons. *Int Rev Neurobiol* 31:145–238
23. Kim Y, Oh HG, Cho YY, Kwon OH, Park MK, Chung S (2016) Stress hormone potentiates Zn^{2+} -induced neurotoxicity via TRPM7 channel in dopaminergic neuron. *Biochem Biophys Res Commun* 470:362–367
24. Yang TC, Wu PC, Chung IF, Jiang JH, Fann MJ, Kao LS (2016) Cell death caused by the synergistic effects of zinc and dopamine is mediated by a stress sensor gene Gadd45b—implication in the pathogenesis of Parkinson's disease. *J Neurochem* 139:120–133
25. Frederickson CJ, Giblin LJ, Krezel A, McAdoo DJ, Muelle RN, Zeng Y, Balaji RV, Masalha R et al (2006) Concentrations of extracellular free zinc (pZn)_e in the central nervous system during simple anesthetization, ischemia and reperfusion. *Exp Neurol* 198:285–293
26. Lee JY, Son HJ, Choi JH, Cho E, Kim J, Chung SJ, Hwang O, Koh JY (2009) Cytosolic labile zinc accumulation in degenerating dopaminergic neurons of mouse brain after MPTP treatment. *Brain Res* 1286:208–214
27. Hirano T, Kikuchi K, Urano Y, Nagano T (2002) Improvement and biological applications of fluorescent probes for zinc, ZnAFs. *J Am Chem Soc* 124:6555–6562
28. Ueno S, Tsukamoto M, Hirano T, Kikuchi K, Yamada MK, Nishiyama N, Nagano T, Matsuki N et al (2002) Mossy fiber $^{2+}Zn^{2+}$ spillover modulates heterosynaptic *N*-methyl-*D*-aspartate receptor activity in hippocampal CA3 circuits. *J Cell Biol* 158:215–220
29. Jackson-Lewis V, Blesa J, Przedborski S (2012) Animal models of Parkinson's disease. *Parkinsonism Relat Disord* 18:S183–S185
30. Rodriguez-Pallares J, Parga JA, Joglar B, Guerra MJ, Labandeira-Garcia JL (2009) The mitochondrial ATP-sensitive potassium channel blocker 5-hydroxydecanoate inhibits toxicity of 6-hydroxydopamine on dopaminergic neurons. *Neurotox Res* 15:82–95
31. Smith RM (2009) NIST critically selected stability constants of metal complexes: version 8. NIST Scientific and Technical Databases [online]. <http://www.nist.gov/srd/nist46.htm>
32. Takeda A, Tamano H, Hisatsune M, Murakami T, Nakada H, Fujii H (2017) Maintained LTP and memory are lost by Zn^{2+} influx into dentate granule cells, but not Ca^{2+} influx. *Mol Neurobiol* 55:1498–1508. <https://doi.org/10.1007/s12035-017-0428-3>
33. Colbourne F, Grooms SY, Zukin RS, Buchan AM, Bennett MV (2003) Hypothermia rescues hippocampal CA1 neurons and attenuates down-regulation of the AMPA receptor GluR2 subunit after forebrain ischemia. *Proc Natl Acad Sci U S A* 100:2906–2910
34. Liu S, Lau L, Wei J, Zhu D, Zou S, Sun HS, Fu Y, Liu F et al (2004) Expression of Ca^{2+} -permeable AMPA receptor channels primes cell death in transient forebrain ischemia. *Neuron* 43:43–55
35. Weiss JH (2011) Ca^{2+} permeable AMPA channels in diseases of the nervous system. *Front Mol Neurosci* 4:42
36. Andrew R, Watson DG, Best SA, Midgley JM, Wenlong H, Petty RK (1993) The determination of hydroxydopamines and other trace amines in the urine of parkinsonian patients and normal controls. *Neurochem Res* 18:1175–1177
37. Jellinger KA, Linert L, Kienzl E, Herlinger E, Youdim MB (1995) Chemical evidence for 6-hydroxydopamine to be an endogenous toxic factor in the pathogenesis of Parkinson's disease. *J Neural Transm Suppl* 46:297–314
38. Sheline CT, Cai AL, Zhu J, Shi C (2010) Serum or target deprivation-induced neuronal death causes oxidative neuronal accumulation of Zn^{2+} and loss of NAD⁺. *Eur J Neurosci* 32:894–904
39. Sheline CT, Zhu J, Zhang W, Shi C, Cai AL (2013) Mitochondrial inhibitor models of Huntington's disease and Parkinson's disease induce zinc accumulation and are attenuated by inhibition of zinc neurotoxicity in vitro or in vivo. *Neurodegener Dis* 11:49–58
40. Sensi SL, Canzoniero LMT, Yu SP, Ying HS, Koh JY, Kerchner GA, Choi DW (1997) Measurement of intracellular free zinc in living cortical neurons: routes of entry. *J Neurosci* 15:9554–9564
41. Colvin RA, Bush AI, Volitakis I, Fontaine CP, Thomas D, Kikuchi K, Holmes WR (2008) Insights into Zn^{2+} homeostasis in neurons from experimental and modeling studies. *Am J Physiol Cell Physiol* 294:C726–C742
42. Blum D, Torch S, Lambeng N, Nissou M, Benabid AL, Sadoul R, Verna JM (2001) Molecular pathways involved in the neurotoxicity of 6-OHDA, dopamine and MPTP: contribution to the apoptotic theory in Parkinson's disease. *Prog Neurobiol* 65:135–172
43. Hyrc K, Handran SD, Rothman SM, Goldberg MP (1997) Ionized intracellular calcium concentration predicts excitotoxic neuronal death: observations with low-affinity fluorescent calcium indicators. *J Neurosci* 17:6669–6677
44. Sensi SL, Ton-That D, Sullivan PG, Jonas EA, Gee KR, Kaczmarek LK, Weiss JH (2003) Modulation of mitochondrial function by endogenous Zn^{2+} pools. *Proc Natl Acad Sci U S A* 100:6157–6162

45. Medvedeva YV, Ji SG, Yin HZ, Weiss JH (2017) Differential vulnerability of CA1 versus CA3 pyramidal neurons after ischemia: possible relationship to sources of Zn²⁺ accumulation and its entry into and prolonged effects on mitochondria. *J Neurosci* 37:726–737
46. Chen Y, Irie Y, Keung WM, Maret W (2002) S-nitrosothiols react preferentially with zinc thiolate clusters of metallothionein III through transnitrosation. *Biochemistry* 41:8360–8367
47. Abiria SA, Krapivinsky G, Sah R, Santa-Cruz AG, Chaudhuri D, Zhang J, Adstamongkonkul P, DeCaen PG et al (2017) TRPM7 senses oxidative stress to release Zn²⁺ from unique intracellular vesicles. *Proc Natl Acad Sci U S A* 114:E6079–E6088
48. Cheramy A, Leviel V, Glowinski J (1981) Dendritic release of dopamine in the substantia nigra. *Nature* 289:537–542
49. Takeda A, Koike Y, Osawa M, Tamano H (2017) Characteristic of extracellular Zn²⁺ influx in the middle-aged dentate gyrus and its involvement in attenuation of LTP. *Mol Neurobiol* 55:2185–2195. <https://doi.org/10.1007/s12035-017-0472-z>
50. Takeda A, Tamano H, Murakami T, Nakada H, Minamino T, Koike Y (2017) Weakened intracellular Zn²⁺-buffering in the aged dentate gyrus and its involvement in erasure of maintained LTP. *Mol Neurobiol*. <https://doi.org/10.1007/s12035-017-0615-2>